

Supporting Information

Carbon Dots with Continuously Tunable Full-Color Emission and Their Application in Ratiometric pH Sensing

Hui Nie,[†] Minjie Li,^{*,†} Quanshun Li,[‡] Shaojun Liang,[‡] Yingying Tan,[‡] Lan Sheng,[†]

Wei Shi,[‡] Sean Xiao-An Zhang^{*,†}

[†]State Key Laboratory of Supramolecular Structure and Materials, College of Chemistry, Jilin University, Changchun 130012, P.R. China

[‡]Key Laboratory for Molecular Enzymology and Engineering of the Ministry of Education, College of Life Science, Jilin University, Changchun 130012, P.R. China

**Correspondence to liminjie@jlu.edu.cn, seanzhang@jlu.edu.cn.*

Materials. CHCl_3 were purchased from Beijing Chemical Company. Diethylamine (DEA), calcium chloride (CaCl_2) and potassium chloride (KCl) were obtained from Xilong Chemical Company. Fluorescein Isothiocyanate (FITC) was purchased from Aladdin Reagent Company. Dulbecco's modified eagle media (DMEM) and fetal bovine serum were obtained from Gibco company. Penicillin (100 $\mu\text{g}/\text{mL}$), streptomycin (100 $\mu\text{g}/\text{mL}$) and 3-(4,5-Dimethylthiazol-2-yl)-2,5-diphenyltetrazolium bromide (MTT) were obtained from Beijing Dingguo Company. LysoTracker@Red DND-99 was obtained from Invitrogen Corporation. Magnesium sulfate (MgSO_4), sodium bicarbonate (NaHCO_3) and glucose were obtained from Beijing Chemical Reagents Company. All the chemicals were used as received without further purification.

Synthesis and purification of fluorescent C dots. For blue fluorescent C dots (B-C dots), the mixture of DEA and CHCl_3 with volume ratio of 1:10 was refluxed for 1 h. Transparent solution was obtained. Then the obtained solutions were dried under vacuum condition, the resulting solid was purified through dialysis to remove the small residues (a membrane with molecular weight cutoff of 3500). For full-color fluorescent C dots (F-C dots), the mixture of DEA and CHCl_3 with volume ratio of 1:10 was refluxed for 60 h, reddish black solution was obtained. For their purification, the solution were dried under vacuum condition, the obtained solids were first purified by dialysis and then separated by column chromatography on silica gel using CH_2Cl_2 : CH_3OH =10:1 as eluent to provide the desired product. Keeping the other synthetic conditions unchanged, C dots with different volume ratio of reactants was also prepared.

Preparation of fluorescein isothiocyanate modified F-C dots (FITC-C dots). Fluorescein isothiocyanate (FITC, 0.1 mg) and purified F-C dots solids (10 mg) were dissolved in 2 mL anhydrous methanol in a flask respectively. Then 2 μL of triethylamine was added to the solution. The mixture was stirred for 24 h at room temperature under dark and then purified through dialysis to remove the unreacted FITC molecule.

Instruments and characterization. Transmission electron microscopy (TEM) was

conducted using a JEM-2100F electron microscope at an acceleration voltage of 200 kV. Fluorescence spectra were measured using a Shimadzu RF-5301 PC spectrophotometer with 1 cm light path cuvettes. The scan step is set as 1 nm. Huber temperature controller was used for the temperature-dependent PL measurements. UV-Vis absorption spectra were measured using a UV-Vis 2550 spectrophotometer with 1 cm light path cuvettes. Fourier transform infrared spectra were recorded on a VERTEX 80/80v spectrometer using the KBr method. Raman spectra were measured with a Renishaw Raman system model 1000 spectrometer with radiation at 633 nm. X-ray Photoelectron Spectroscopy (XPS) was investigated by using ESCALAB 250 spectrometer with a mono X-ray source Al K α excitation (1486.6 eV). Elemental analysis was performed on Elementar Vario MICRO CUBE, each data was parallel at least twice. The confocal fluorescence images of F-C dots and FITC-C dots labeled cells were acquired with a fluorescence confocal microscope (Zeiss LSM 710, Germany) under ambient conditions. And the images were collected using a diode laser at 405 nm as the excitation source. The absorbance for MTT analysis was recorded on a microplate reader (BIO-TEK Synergy HT, USA) at 490 nm. $^1\text{H-NMR}$ and $^{13}\text{C-NMR}$ spectra were obtained using Varian 300M. High resolution mass spectrometry (HRMS) data were obtained using Agilent 1290- microTOF QII. The fluorescence lifetime were measured on FLS 920 lifetime and steady state spectrometer. The fits of the fluorescence decay traces for B-C dots, F-C dots and reduced F-C dots reach acceptable residuals ($\chi^2 \approx 1.1$). The intensity-weighted average lifetime (τ_{av}), the mean time delay of photon emission after the picosecond laser pulse, was calculated according to

$$\tau_{\text{av}} = \frac{\sum \alpha_i \tau_i^2}{\sum \alpha_i \tau_i}$$

where the α_i represent the fractional weights of the various decay time components, τ_i of the multi-exponential fitting.

Cell culture and fluorescence imaging. The HeLa cells were grown on glass-bottom culture dishes (MatTek Co.) in Dulbecco's modified eagle media (DMEM) supplemented with 10% (v/v) fetal bovine serum, penicillin (100 $\mu\text{g/mL}$), and

streptomycin (100 µg/mL) at 37 °C in a 5% CO₂ incubator. For fluorescence imaging, the adherent cells were incubated with F-C dots and FITC-C dots (20 µg/mL) for 2 h at 37 °C. Control experiment was also done at 4 °C to determine the way of FITC-C dots entering cells. Before use, the adherent cells were washed three times with PBS (pH 7.4) to remove the excess F-C dots and FITC-C dots. Fluorescence imaging experiments were performed on a fluorescence confocal microscope (Zeiss LSM 710) under ambient conditions. The confocal fluorescence images were collected using a diode laser at 405 nm as the excitation source. A Plan-Apochromat 20×/0.8 M27 and 63×/1.40 Oil M27 objectives were utilized for imaging and spectral data acquisition.

For co-localization experimentation, the cells were incubated with 2 mL DMEM containing FITC-C dots (20 µM) and LysoTracker@Red DND-99 (0.13 µM) in an atmosphere of 5% CO₂ and 95% air for 2 h at 37 °C. The cells were washed for three times with PBS at room temperature. The confocal fluorescence images were collected using diode lasers at 405 nm and 543 nm as the excitation sources. A 63×/1.40 Oil M27 objective lens was utilized for imaging.

Cytotoxicity assay. The cytotoxicity of F-C dots is evaluated by the standard MTT assay. Briefly, HeLa cells were seeded in 96-well U-bottom plates at a density of 7000 cells/well, and incubated with F-C dots at varied concentrations (0-20 µg/mL) at 37 °C for 24 h. Then, the culture media were discarded, and 0.02 mL of the MTT solution (5 mg/mL in DMEM) was added to each well, followed by incubation at 37 °C for 4 h. The supernatant was abandoned, and 150 µL of DMSO was added to each well to dissolve the formed formazan. After shaking the plates for 10 min, absorbance values of the wells were measured with a microplate reader at 490 nm. The cell viability was calculated according to the equation: cell viability = $A/A_0 \times 100\%$, where A is the absorbance of the experimental group (i.e., the cells were treated by F-C dots) and A₀ is the absorbance of the control group (i.e., the cells were untreated by F-C dots).

Quantum yields (QY) measurements. Reference on quantum yields measurements: Lakowicz, J. R. *Principles of Fluorescence Spectroscopy*, 2nd Ed., 1999, Kluwer

Academic/Plenum Publishers, New York. Fluorescence quantum yield was measured by using anthracene in ethanol ($\Phi_F = 0.27$) for B-C dots and Rhodamine B in ethanol ($\Phi_F = 0.89$) for F-C dots as fluorescence standards. The absorbance of the sample in ethanol solution at the excitation wavelength (optical density < 0.1 to minimize inner-filter effects) was matched with the standard.

The quantum yield was calculated using the below equation:

$$\varphi_x = \varphi_{std} \left[\frac{I_x}{A_x} \right] \left[\frac{A_{std}}{I_{std}} \right] \left[\frac{\eta_x}{\eta_{std}} \right]^2$$

Where φ is the quantum yield, I is the measured integrated emission intensity, and A is the optical density, and η the refractive index. The subscript “*std*” refers to the reference fluorophore of known quantum yield.

Table S1 PL properties of F-C dots

λ_{ex} (nm)	λ_{em} (nm)	$\Delta\lambda$ (nm)	FHWM ^a (nm)	Intensity
390	472	82	136	52.5
430	493	63	129	64.3
470	542	72	106	84.3
510	548	38	72	149.2
530	555	25	—	160.9
570	600	30	—	110.4
610	647	37	—	121.6
630	660	30	—	130.3
650	671	21	—	124.2

^a FWHM = full width at half maximum; $\Delta\lambda = \lambda_{em} - \lambda_{ex}$.

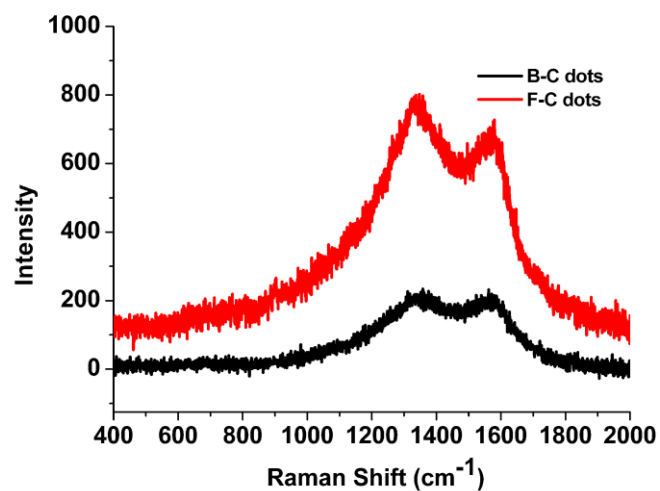


Figure S1. Raman spectra of the B-C dots and F-C dots, respectively.

Table S2 XPS analysis of C 1s in B-C dots and F-C dots

	C-C (284.7 eV) (%)	C-N (285.6 eV) (%)	C-O (286.0 eV) (%)	C=O/C=N (287.4 eV) (%)
B-C dots	71.2	5.4	19.1	4.3
F-C dots	67.3	9.8	13.7	9.2

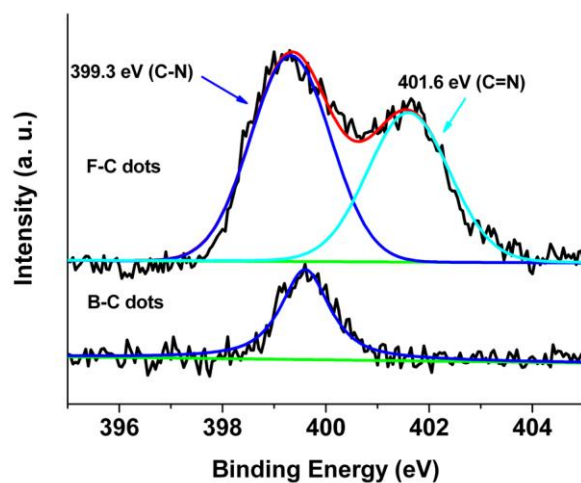


Figure S2. High-resolution XPS spectra of the N 1s of B-C dots and F-C dots, respectively.

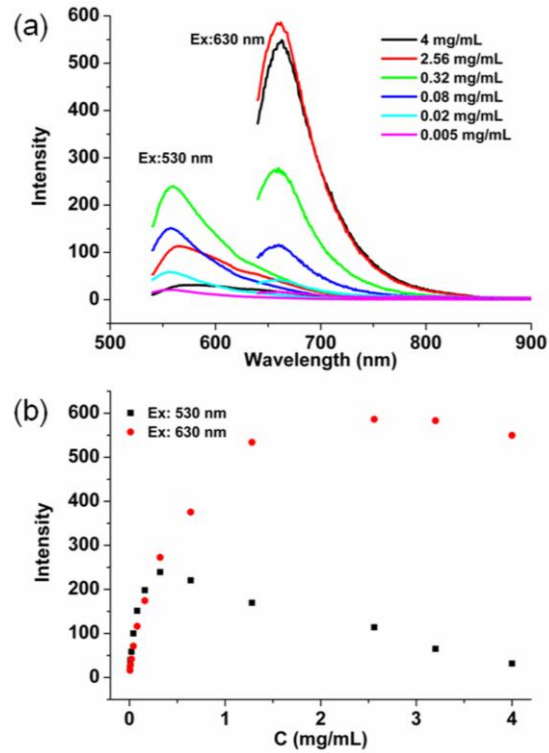


Figure S3. (a) Fluorescence spectra of F-C dots in ethanol with different concentrations under excitation wavelengths of 530 nm and 630 nm; (b) Emission intensity variations at peak positions of F-C dots in ethanol with different concentrations.

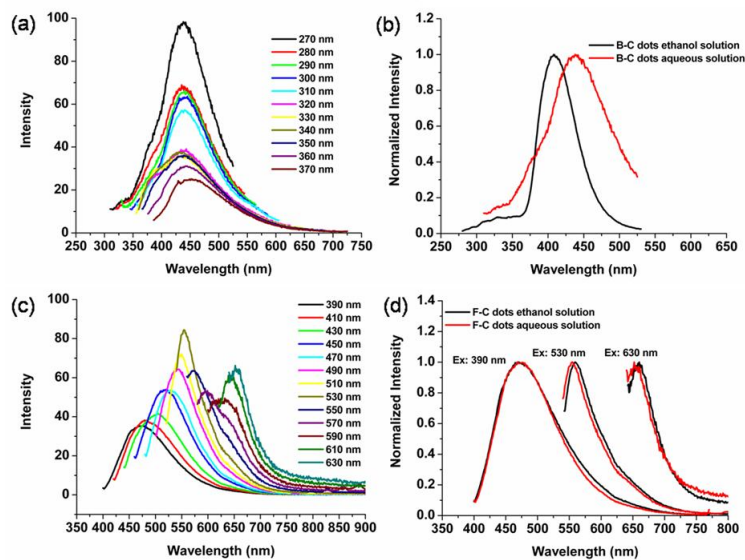


Figure S4. (a, c) Fluorescence spectra of B-C dots (0.0125 mg/mL) and F-C dots (0.018 mg/mL) in water, respectively; (b, d) Comparison of the fluorescence spectra

in water and ethanol for B-C dots (λ_{ex} : 270 nm) and F-C dots (λ_{ex} : 390 nm, 530 nm and 630 nm), respectively.

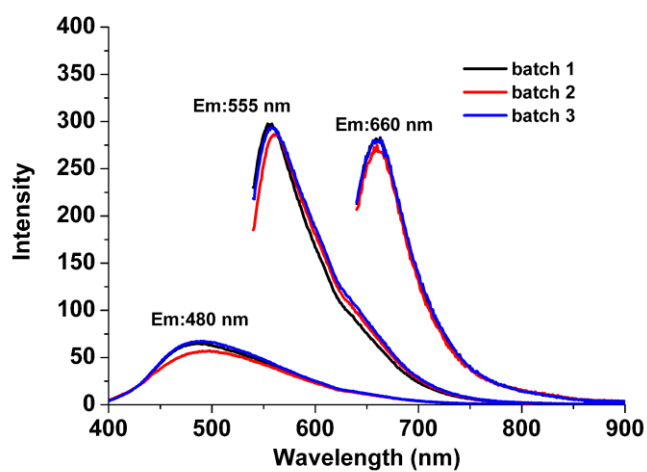


Figure S5. Comparison of the fluorescence spectra of three parallel batches of C dots in ethanol (reaction time: 60 h, dialysed).

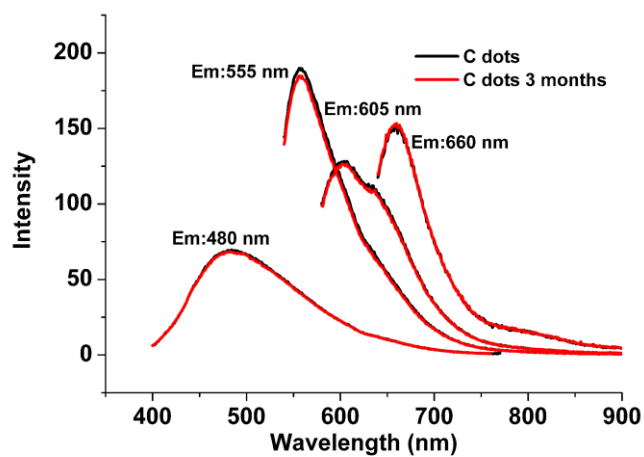


Figure S6. Fluorescence spectra of fresh C dots and C dots after three months of storage.

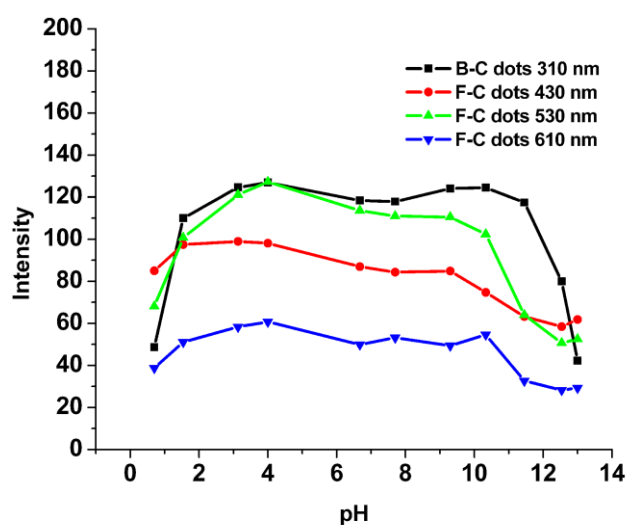


Figure S7. Plots of the emission intensity at 310 nm of B-C dots and 430 nm, 530 nm and 610 nm of F-C dots as a function of pH.

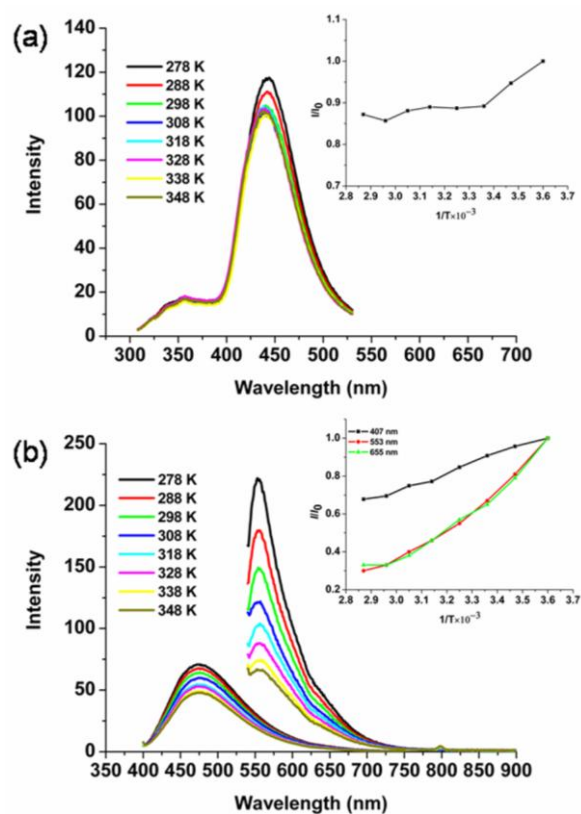


Figure S8. (a) Fluorescence intensity of B-C dots in aqueous solution at emission wavelength of 439 nm; Inset of (a): Arrhenius plot of the thermal PL quenching of B-C dots, I_0 and I are PL intensities recorded at 278 K and at higher temperature

points, respectively. (b) Fluorescence intensity of F-C dots in aqueous solution as a function of temperature between 278 K and 348 K (λ_{em} : 470 nm, 553 nm and 655 nm); Inset of (b): Arrhenius plot of the thermal PL quenching of F-C dots.

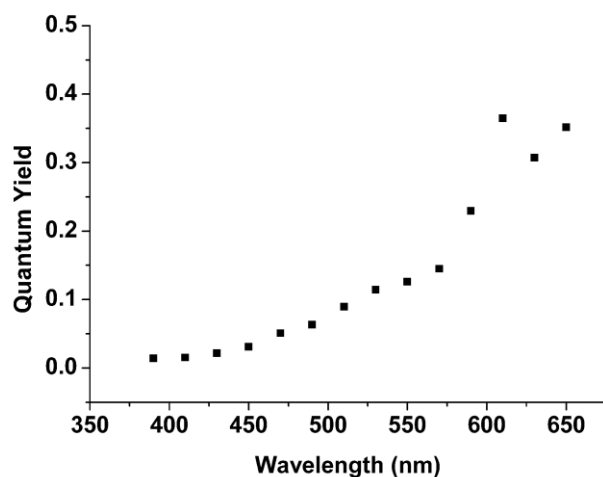


Figure S9. Approximate quantum yields of F-C dots calculated at different emission wavelengths. The QY of F-C dots at different wavelengths were calculated using itself (QY measured with excitation wavelength of 550 nm) as reference. When the F-C dots were excited with long wavelength light, emission band with asymmetric shape were obtained. Then integrated emission intensity (peak area) can hardly measured, here, the emission intensity value were used to calculate the QY. The QY of F-C dots increase with the redshift of excitation wavelengths and the maximum QY occurs near 600 nm, then decline at wavelengths longer than 600 nm.

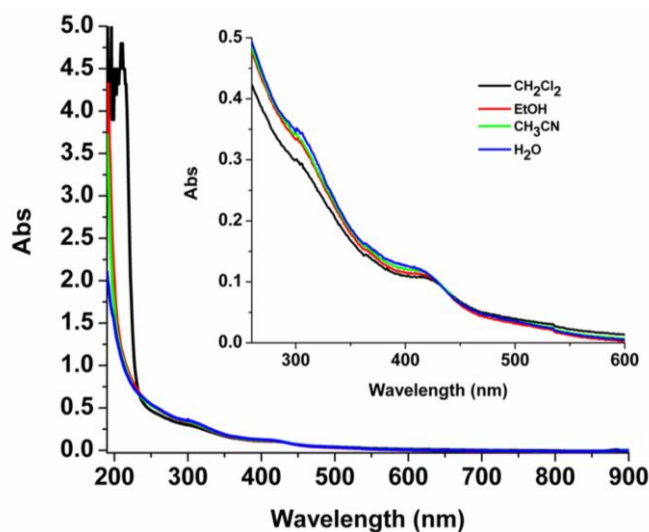


Figure S10. Solvent-dependent UV-visible absorption spectra of F-C dots.

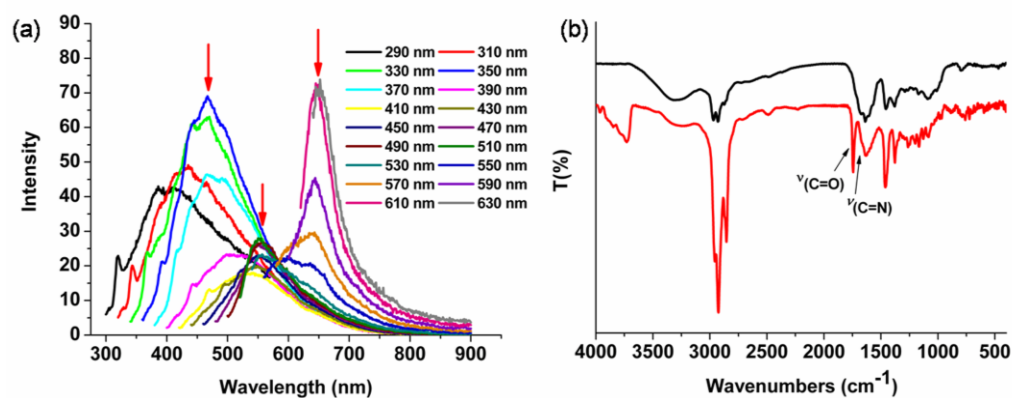


Figure S11. (a) Fluorescence spectra of C dots (volume ratio of CHCl_3 and DEA=1:2) in ethanol under different excitation wavelengths; (b) FT-IR spectra of C dots (red curve: F-C dots; black curve: C dots with volume ratio of CHCl_3 and DEA=1:2).

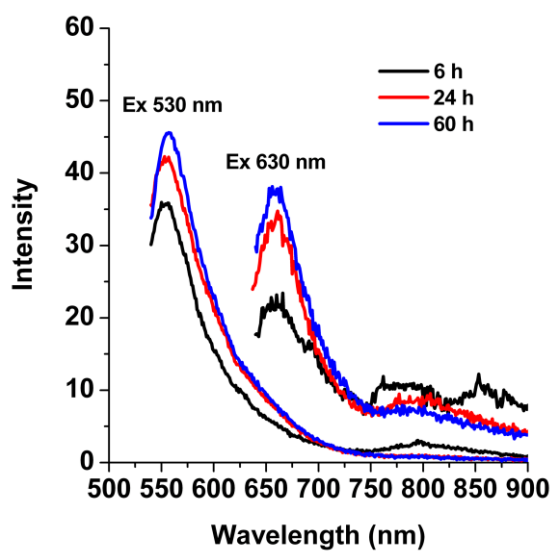


Figure S12. Fluorescence spectra of C dots with reaction time of 6 h, 24 h and 60 h, respectively (λ_{ex} : 530 nm and 630 nm).

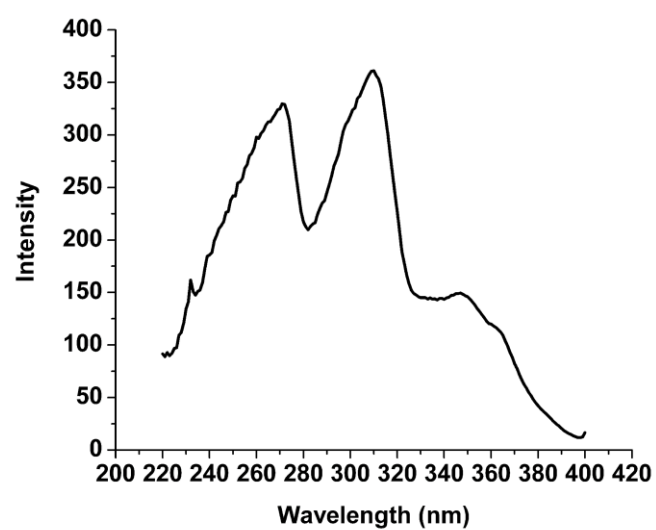


Figure S13. Fluorescence excitation spectra of B-C dots monitored at maximum emission wavelength of 407 nm.

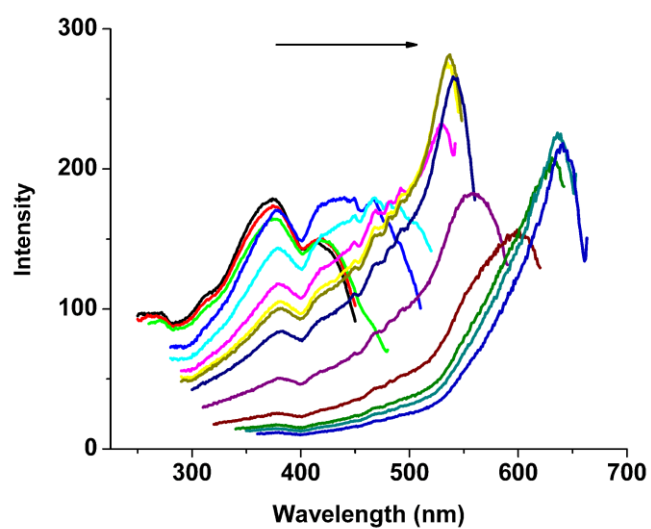


Figure S14. Fluorescence excitation spectra of F-C dots monitored at different emission wavelengths as shown in Figure 1d.

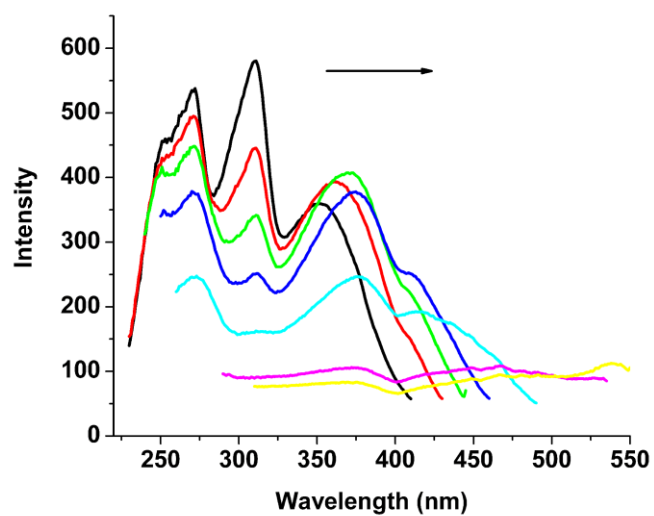
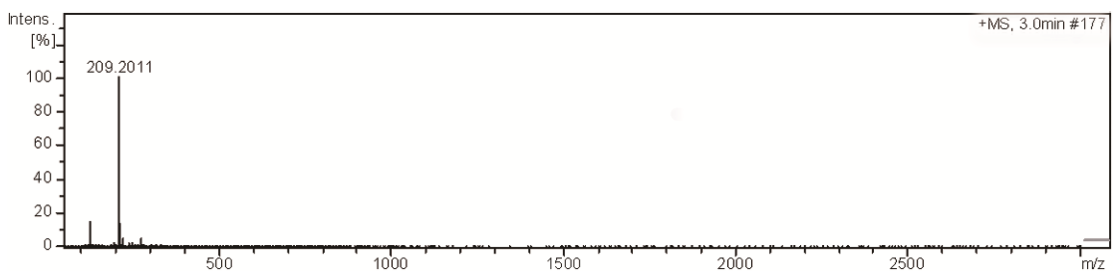
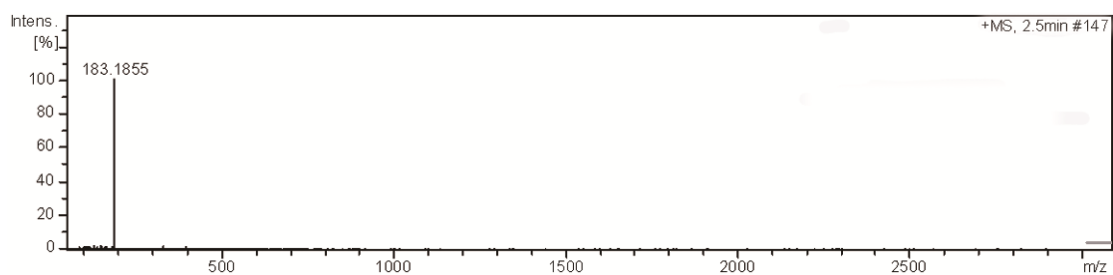


Figure S15. Fluorescence excitation spectra of reduced F-C dots monitored at different emission wavelengths as shown in Figure 4c.

Structural characterization of diethylammonium chloride: $^1\text{H-NMR}$: (300 MHz, CDCl_3) $\delta = 9.52$ (2H, s), 3.02 (4H, q, $J=7.3$ Hz), 1.47 (6H, t, $J=7.3$ Hz); HRMS: calcd. for $[\text{2M-Cl}]^+$: 183.1627 [M: $\text{NH}_2(\text{C}_2\text{H}_5)_2\text{Cl}$]; found 183.1627: $[\text{2M-Cl}]^+$.



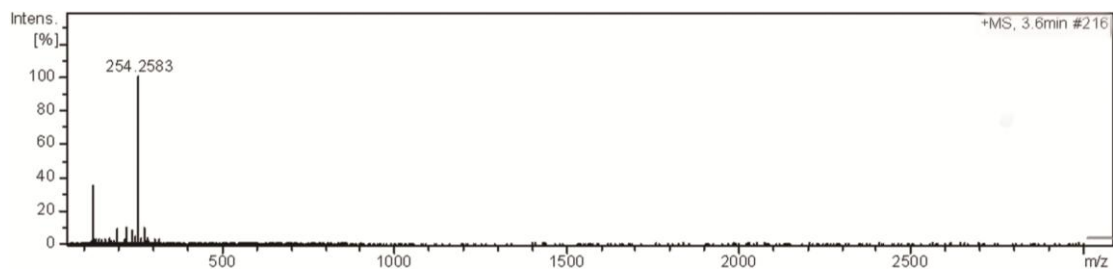


Figure S16. LC-HRMS spectra of the small molecules generated during the reaction of CHCl_3 and DEA.

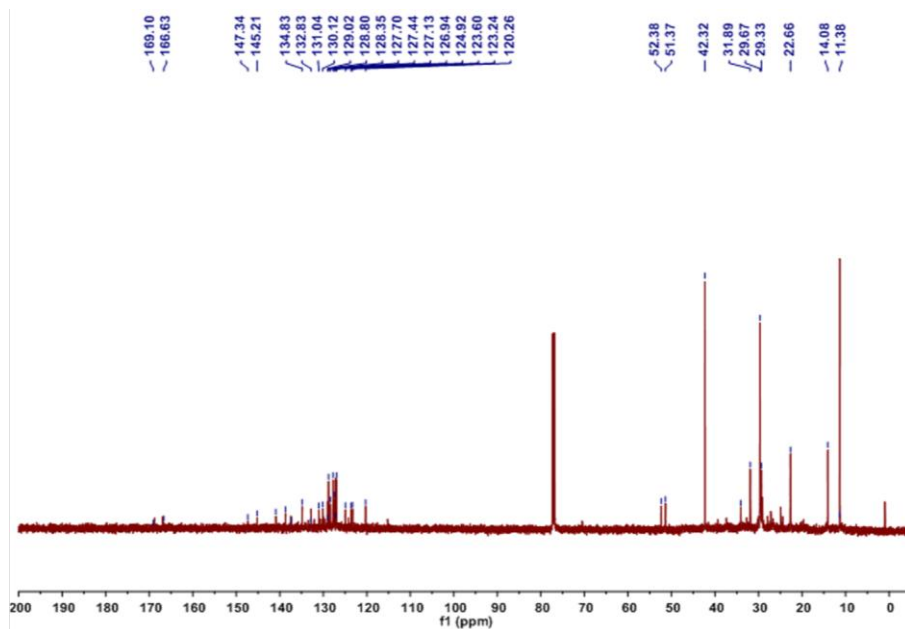


Figure S17. ^{13}C -NMR spectrum of C dots in CDCl_3 showing the presence of fused ring structures with signals in the $\delta=110\text{--}180$ ppm range.

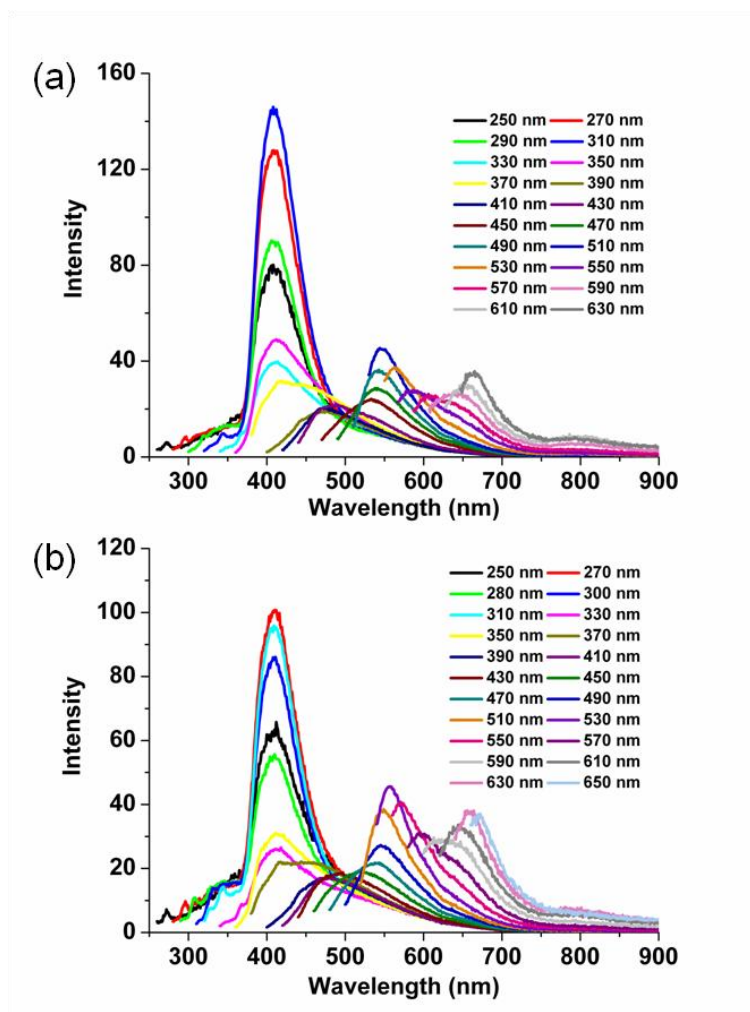


Figure S18. Fluorescence spectra of C dots reacted for 24 h (a) and 60 h (b) (purified by dialysis) respectively under different excitation wavelength.

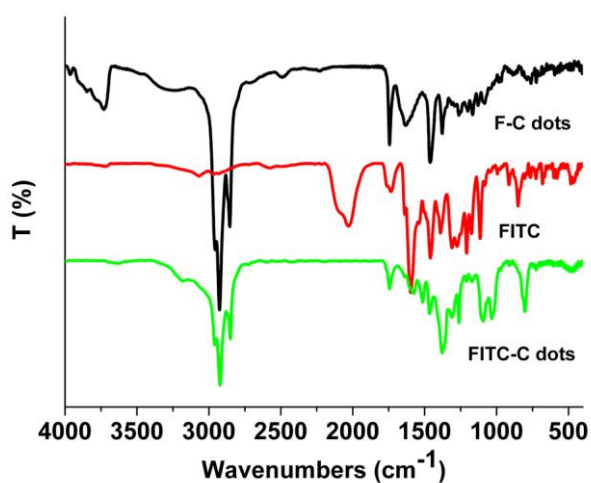


Figure S19. FT-IR spectra for F-C dots, FITC and FITC-C dots respectively. The peaks at 1741 cm^{-1} for carboxyl group and 1600 cm^{-1} for vibration of C=C in the

aromatic ring of pure FITC exist in FITC-C dots, and the peak for $-S=C=N$ at 2034 cm^{-1} disappeared in FITC-C dots. IR spectra show that FITC has been conjugated to F-C dots.

Calculation of the amounts of FITC conjugated to F-C dots. The concentration of FITC was determined by fluorometric method. Different concentrations of FITC methanol solutions were made, all of which had absorbance less than 0.1 at 493 nm. A Shimadzu RF-5301 PC spectrophotometer with an excitation slit width of 1.5 and an emission slit width of 1.5 was used to excite the samples at 500 nm and to record their photoluminescence spectra. The data of photoluminescence intensity was plotted and the slope of the standards was determined. The data showed good linearity. Then the concentration of the FITC in dialysate can be calculated with the obtained standard curve.

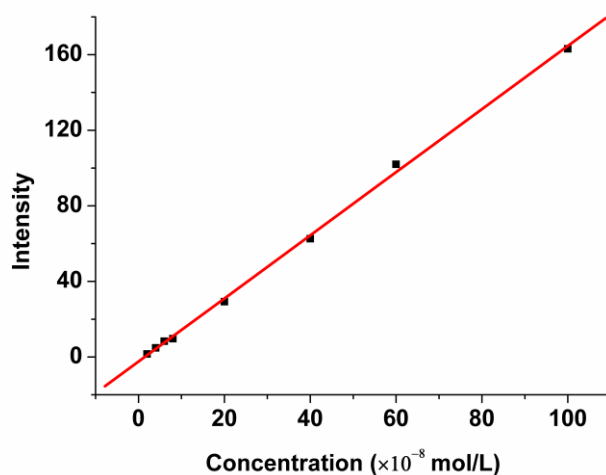


Figure S20. Plot of photoluminescence intensity of FITC with different concentrations. Then the concentration of FITC residues in dialysate can be determined and the amount of FITC linked to F-C dots can be calculated.

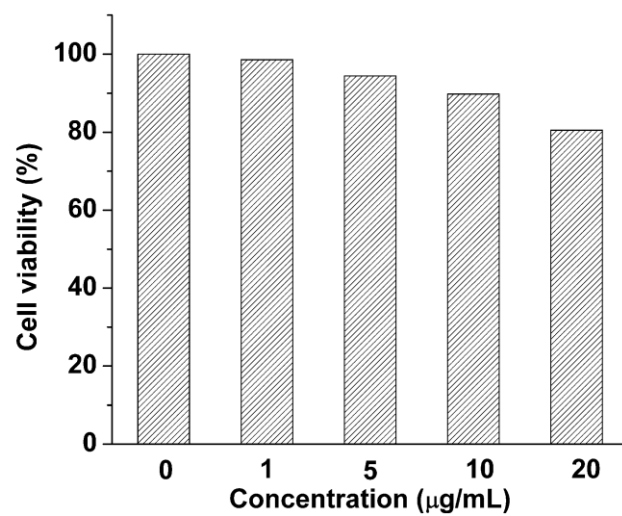


Figure S21. Effects of F-C dots at varied concentrations on the viability of HeLa cells.

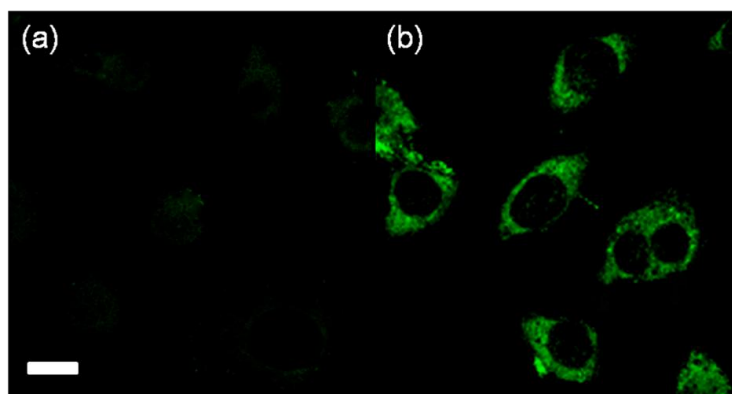


Figure S22. Confocal images of HeLa cells after incubation with FITC-C dots at (a) 4 °C and (b) 37 °C. The images are collected in the ranges of 500–540 nm at $\lambda_{\text{ex}} = 405$ nm; Scale bar = 20 μm .

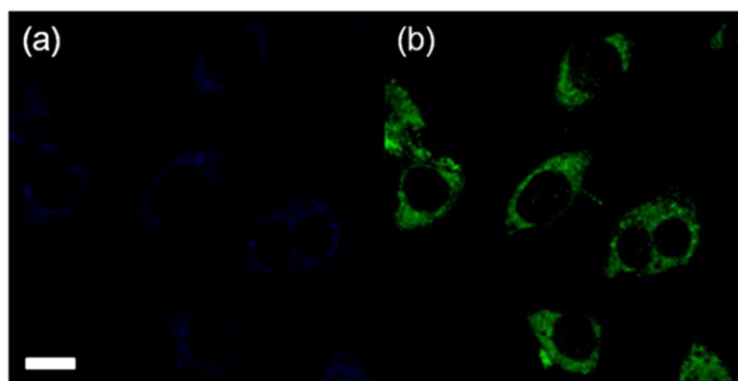


Figure S23. Fluorescent images of HeLa cells labeled by FITC-C dots. The image of (a) is collected in the ranges of 440–480 nm at $\lambda_{\text{ex}} = 405$ nm (channel a); The image of (b) is collected in the ranges of 500–540 nm at $\lambda_{\text{ex}} = 405$ nm (channel b); Scale bar = 20 μm .

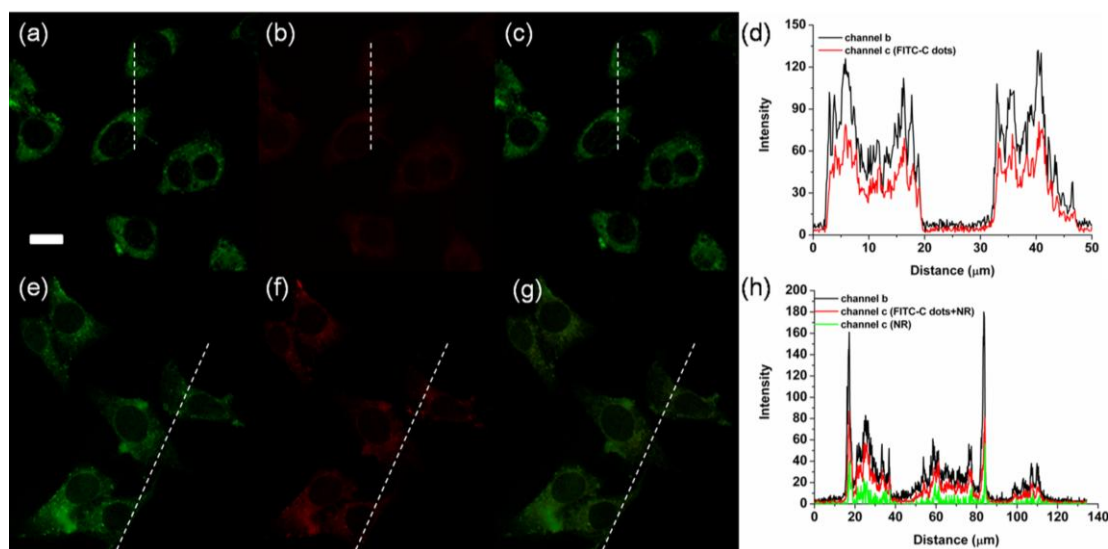


Figure S24. Fluorescent images of HeLa cells stained with FITC-C dots (a-c) and co-incubated with FITC-C dots and LysoTracker@Red DND-99 (e-g). The images of (a) and (e) are collected in the ranges of 500–540 nm at $\lambda_{\text{ex}} = 405$ nm (channel b); The images of (b) and (f) are collected in the ranges of 610–650 nm at $\lambda_{\text{ex}} = 543$ nm (channel c); The images of (c) is the overlay of (a) and (b), (g) is the overlay of (e) and (f); (d and h) are intensity profile of regions of interest across HeLa cells; Scale bar = 20 μm . As FITC-C dots feature full-color emission across the whole visible range, fluorescence signal of LysoTracker@Red DND-99 in red region (channel c: $\lambda_{\text{ex}} = 543$ nm, $\lambda_{\text{em}} = 610$ –650 nm) was perturbed. When the HeLa cells were stained with FITC-C dots only, the intensity of channel b to c varies synchronously (FITC-C dots) with high Pearson's coefficient of 0.91 (Figure S24d). Thus the fluorescence intensity from LysoTracker@Red DND-99 can be obtained approximately by subtraction of the overlapping signals from FITC-C dots.

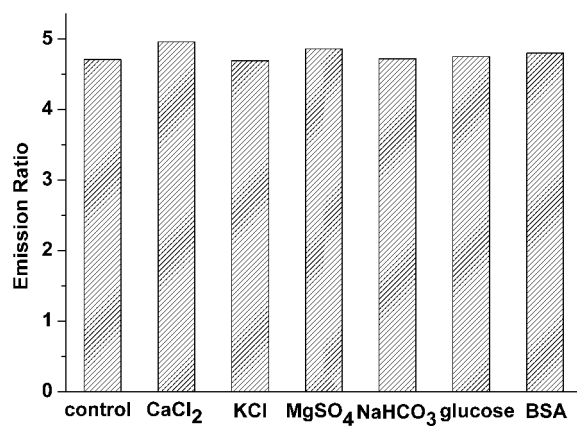


Figure S25. Effects of intracellular species (2 mM CaCl₂, 150 mM KCl, 2 mM MgSO₄, 10 mM NaHCO₃, 20 mM glucose and 1 mM bovine serum albumin) on the fluorescence intensity ratio of FITC-C dots.